2015-2016 NASA Student Launch

Alabama Rocket Engineering Systems (ARES) Team

Motor Change Addendum

April 2016

Table of Contents

1. Overview

1.1 Initial Reasons for Change

The Alabama Rocket Engineering Systems (ARES) team initially changed the motor selection to a Cesaroni Pro75 3683L851-P, (L851), after careful consideration of the risks to the vehicle and team. The ARES team initially changed the selection due to fear of a motor CATO with a motor that required bonding, NASA's requirement of additional weight to correct the stability margin during the Critical Design Report, (CDR), and the knowledge that a longer-burning motor is more reliable than a fast-burning.

Due to a shipping mishap the ARES team initially tested the full scale launch vehicle with the L851 at Talladega, AL on February 20. After observing University of Alabama at Huntsville's motor fall victim to catastrophic over-pressurization, (CATO), at Talladega the team was concerned about testing the Cesaroni Pro75 3300L3200-P, (L3200), because the L3200 is a fast-burning motor, 1.03 (sec), that requires bonding. It would be very unforgiving to the vehicle if bonded improperly. Fortunately, the L3200 performed its function adequately. However, after observing Auburn University experience a CATO for the second time at Manchester, TN on March 5, and when both motors observed required bonding ARES became exceptionally uncomfortable with using a motor requiring bonding. Not only would a CATO mean endangering observers on the field it would also mean a catastrophic loss of the payload and launch vehicle, a monetary loss of over $6000, and ARES dreams of winning the competition and hard work of over a year would, quite literally, go up in flames.

During the CDR, ARES was asked to add weight to further correct the static stability margin off the rail. The expected static stability margin at rail exit at the CDR was 1.66 calibers. After completion of the full scale launch vehicle and addition of weight to the nose cone the rail exit static stability margin was raised to 2.02 calibers. At the time, the ARES team felt that with the addition of the weight and the long-burning characteristics of the L851, 4.34 (sec), the L851 was a better choice.

The flight altitude and speed off of the launch rail produced by the L851 are likely to be more consistent than the L3200 because of the higher burn stability, (motor stability) of the L851 and the higher instability of the burn of the L3200. The likelihood of a CATO also decreases with the L851 because the motor is more stable.

1.2 Considerations and Analysis of Motor Choices

Initially, the ARES team only considered the L3200 and the L851 because they were both flight-tested and proven adequate. After the Flight Readiness Review, (FRR), Presentation, the ARES team was asked to consider all similar motor options available before submitting the final motor selection as an addendum to the FRR. All motors considered are presented in Table 1.2.1.

Motor Considered	Bonding Required	Availability
Cesaroni L3200	Yes	No
Cesaroni L851	No	Yes
Cesaroni L1050	No	Yes
Cesaroni L800	No	Yes

Table 1.2.1 Motor Selection Study

ARES already had submitted the order and paid for a Cesaroni L851 from Chris' Rocket Supplies, Chris Short. ARES plans to try utilize Chris Short to "switch," motors if a new motor is selected especially since ARES already has a monetary commitment and a relationship with Chris Short. Chris has been invaluable to ARES with his flexibility, advice, and general helpfulness. Both Lee Brock and Chris Short felt that out of the original two motors selected the L851 was the safer choice.

If a new motor was selected, NASA requested: the trajectory off the rail, static stability off of the rail, a thrust to weight ratio of about 5, and an advantageous rail velocity. The ARES team also chose to include in its consideration: the change in weight of the launch vehicle throughout the motor burn, the Thrust to Weight ratio, (T/W), change throughout the motor burn, the center of gravity, (CG), change from the motor burn, how the HAL payload emergency safety changes will affect the flight of the launch vehicle, the CATO history of each motor, and the simulated and actual altitude of the launch vehicle with each motor.

1.3 Final Motor Choice Pending NASA Approval

After careful consideration, the Cesaroni L851 is the safest choice for the ARES team. As will be shown in the following sections; ARES is confident NASA will agree. All elements of the motor study are listed in Table 1.3.1. ARES considered the availability of the motors, the change in weight of the launch vehicle, the T/W, and the CG change and its effect on the static stability margin during the motor burn, how the HAL payload emergency safety changes will affect the launch vehicle flight, the history of each motor was considered, the trajectory, static stability, and T/W off of the rail, the rail exit velocity, and the simulated and actual altitude.

Elements	L3200	L851	L1050	L800
Availability	No	Yes	Yes	Yes
Bonding	Yes	No	No	No
Burn Time	1.03 sec	4.34 sec	3.56 sec	4.67 sec
Tested on Launch Vehicle	Yes	Yes	No	No
Static Stability Margin Off Rail (3>SSM>2)	2.14	2.04	2.06	2.04
Static Stability Margin After Burnout	2.66	2.66	2.64	2.59
Rail Trajectory (15 mph)	2.46 deg.*	5.29 deg.	5.04 deg.	4.83 deg.
Altitude of Flight Expected to be Under 5600 ft	Yes	Yes	No	No

Table 1.3.1 Overview of Findings of Motor Study

*The calculated value violates assumptions made. See the specific section for more information.

From Table 1.3.1, the L851 is the only motor that meets all safety requirements.
As is it is shown in Table 1.3.1; not only is the L851 the best option available to the ARES team, it is also the only motor available that is flight-tested and proven on the ARES launch vehicle. ARES is confident that NASA will concur that the L851 is the best choice after examining the study and its conclusions.

2. HAL Payload Emergency Safety Changes Effects on Launch Vehicle

The HAL payload's decision to remove the lander legs after failed testing alleviated concerns on the launch vehicle design team of potentially catching and tangling with the drogue parachute on ejection if the legs prematurely deployed.

The decision to remove the legs forces the launch vehicle team to add weight in order to least maintain the static stability margin above 2 calibers. The lander legs added about 3 lb to the launch vehicle during flight.

Two solutions were presented:

1. Add 1 lb of ballast weight to the payload and 2.2 lb to the nose cone.
2. Add 3 lb of ballast weight to the payload.

As a review, the state of the launch vehicle with all motors in the study considered is presented in Table 2.1. The thrust to weight ratio, T/W, is taken as the average thrust over the liftoff weight per NAR requirements.

Motor	Weight (lb)	Avg Thrust (lb)	Max Thrust (lb)	T/W	Burn time (s)	Stabilty Margin	Altitude	Bonding?	Available?
L851	38.4	190.9	222.5	4.971354167	4.3	2.14	4874	No	Yes
L3200	37.2	721.5	837.9	19.39516129	1	2.3	4566	Yes	No
L1050	37.6	235.2	271.7	6.255319149	3.6	2.24	5170	No	Yes
L800	37.7	180.7	289.1	4.793103448	4.7	2.23	5069	No	Yes

Table 2.1 Launch Vehicle Pre-Payload Safety Change

The altitude considered in Table 2.1 is simulated at Bragg Farms on OpenRocket. Consideration was given to Solution 1, Table 2.2, and Solution 2, Table 2.3, as to which provided the best static stability margin update, kept the altitude simulated as close as possible, provided the best rail exit conditions, and which was the easiest to accomplish.

Motor	Weight (lb)	Avg Thrust (lb)	Max Thrust (lb)	T/W	T/W off pad	Stability Margin	Altitude
L851	37.6	190.9	222.5	5.10	5.71	2.14	5018 ft
L3200	36.4	721.5	837.9	19.8	16.7	2.3	4684 ft
L1050	36.8	235.2	271.7	6.39	5.96	2.21	5311 ft
L800	36.9	180.7	289.1	4.89	5.29	2.19	5215 ft

Table 2.2 1 lb of ballast weight to the payload and 2.2 lb to the nose cone

Motor	Weight (lb)	Avg Thrust (lb)	Max Thrust (lb)	T/W	T/W off pad	Stabilty Margin	Altitude
L851	37.4	190.9	222.5	5.10	5.74	2.13	5054 ft
L3200	36.2	721.5	837.9	19.93	16.83	2.29	4714 ft
L1050	36.6	235.2	271.7	6.42	5.98	2.24	5346 ft
L800	36.7	180.7	289.1	4.92	5.31	2.22	5252 ft

Table 2.3 3 lb of ballast weight to the payload

Based off Table 2.2 and Table 2.3 the results are similar with the only difference being a slight increase in predicted altitude for Solution 2. Solution 1 was chosen because there were concerns brought up about any weight added inside the payload bay runs the risk of damaging components. Solution 1 was a compromise between adding 3 lb directly to the nose cone and 3 lb to the payload. Adding 3 lb directly to the nose cone was dismissed based on concerns of over-weathercocking and load added to the bulkhead. Solution 1's simulated data will be examined for the motor study along with previous flight information.

3. Motor Study

Despite its non-availability for purchase the ARES team considered the flight characteristics of the L3200 in the study. Rather than an exercise in futility, the ARES team felt it was important to show that the motor had been considered, despite the team concerns over bonded fast-burning motors, and was found to be unavailable.

3.1 Motor Characteristics

Four motors were considered in this motor study. The Cesaroni L3200, L851, L1050, and the L800. The motors initial and final weight, average and max thrust, burn duration, and total impulse are included in Table 3.1.1.

Motors	W (lbf): Initial, Final	Efficiency (%)	T (lbf): Average, Max	Burn Duration (sec)	I (lb*sec)
L3200	7.20, 3.54	50.81%	721.5, 837	1.03	741.9
L851	8.36, 3.52	57.93%	190.9, 222.5	4.34	828.0
L1050	7.61, 3.51	54.05%	235.2, 271.7	3.56	837.9
L800	7.75, 3.61	53.35%	180.9, 289.36	4.67	845.33

Table 3.1.1 Relevant Data for Motor Study [1]

The L3200 exerts the most thrust force but only over about 1 second of burn time. The launch vehicle structure will experience the highest load from this motor and is the most inefficient which is typical of a fast-burning highly-reactive motor. The launch vehicle will be in glide to the altitude desired after the 1 second burn making this flight the most dependent on atmospheric conditions. The L3200 requires bonding.

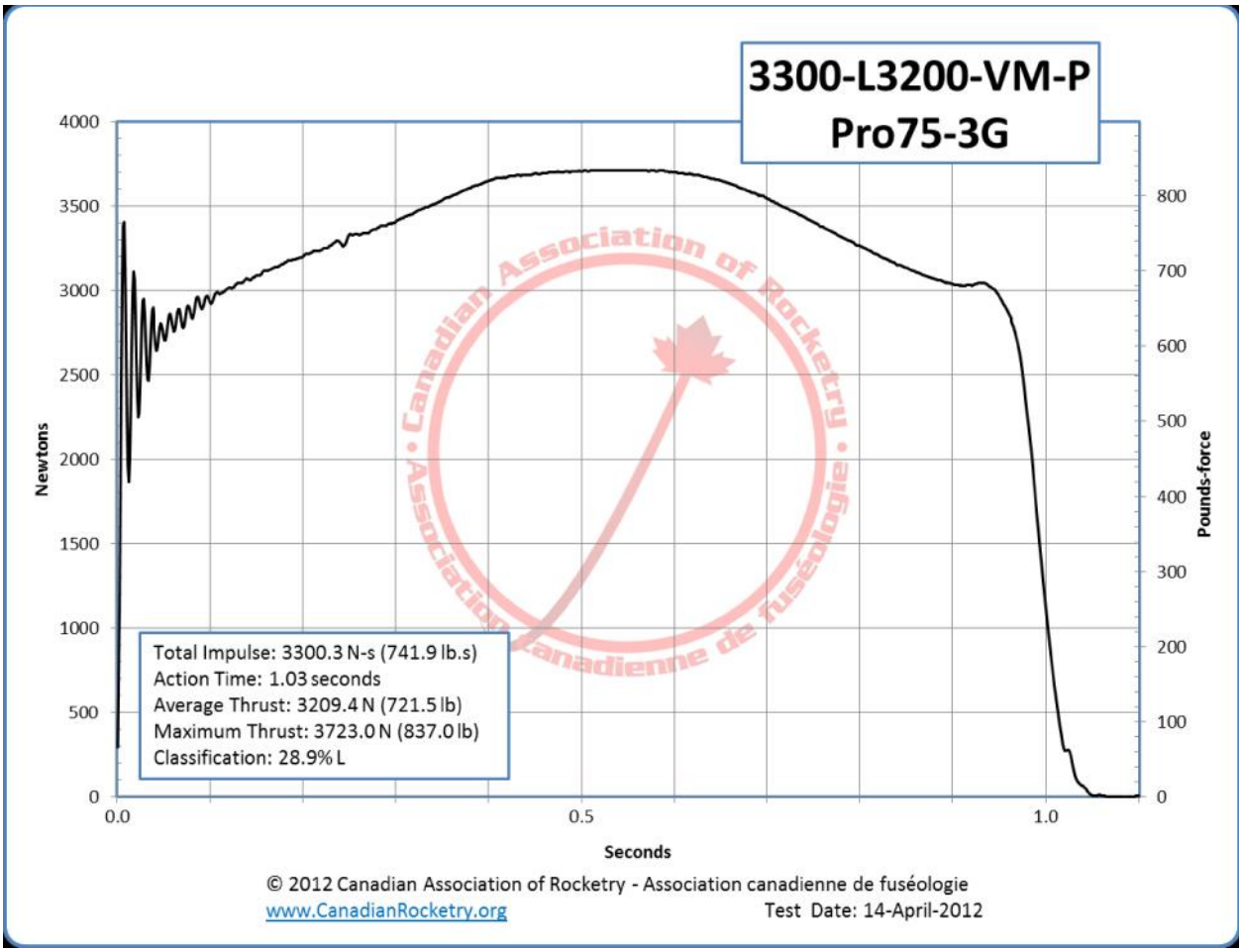

Figure 3.1.1 Thrust Curve for L3200 [1]

The L3200 thrust curve, Figure 3.1.1, shows that the L3200 has the largest variation in thrust from ignition to the thrust off the pad to flight, 200 lb and 150 lb, respectively. This is typical of a fast-burning highly-reactive motor. The time off the launch rail simulated is 0.22 sec. The actual time off the launch rail from the flight at Manchester was 0.25 sec, with an error margin of 0.05 sec, which shows good agreement with the simulation. The pre-payload safety change simulated altitude was 4566 ft with an actual altitude of 4876 ft achieved at Manchester, TN. The atmospheric conditions will be discussed in Section 3.1.1.

The L851 is the most efficient motor, 57.93%, with the second longest burn time. With a burn time of 4.34 sec, only 0.33 sec less than the longest burn, the L851 exerts the least amount of impact on the structure for the best amount of thrust. The L851 as a long-burning stable motor is one of the more reliable motors in the study. The L851 does not require bonding.

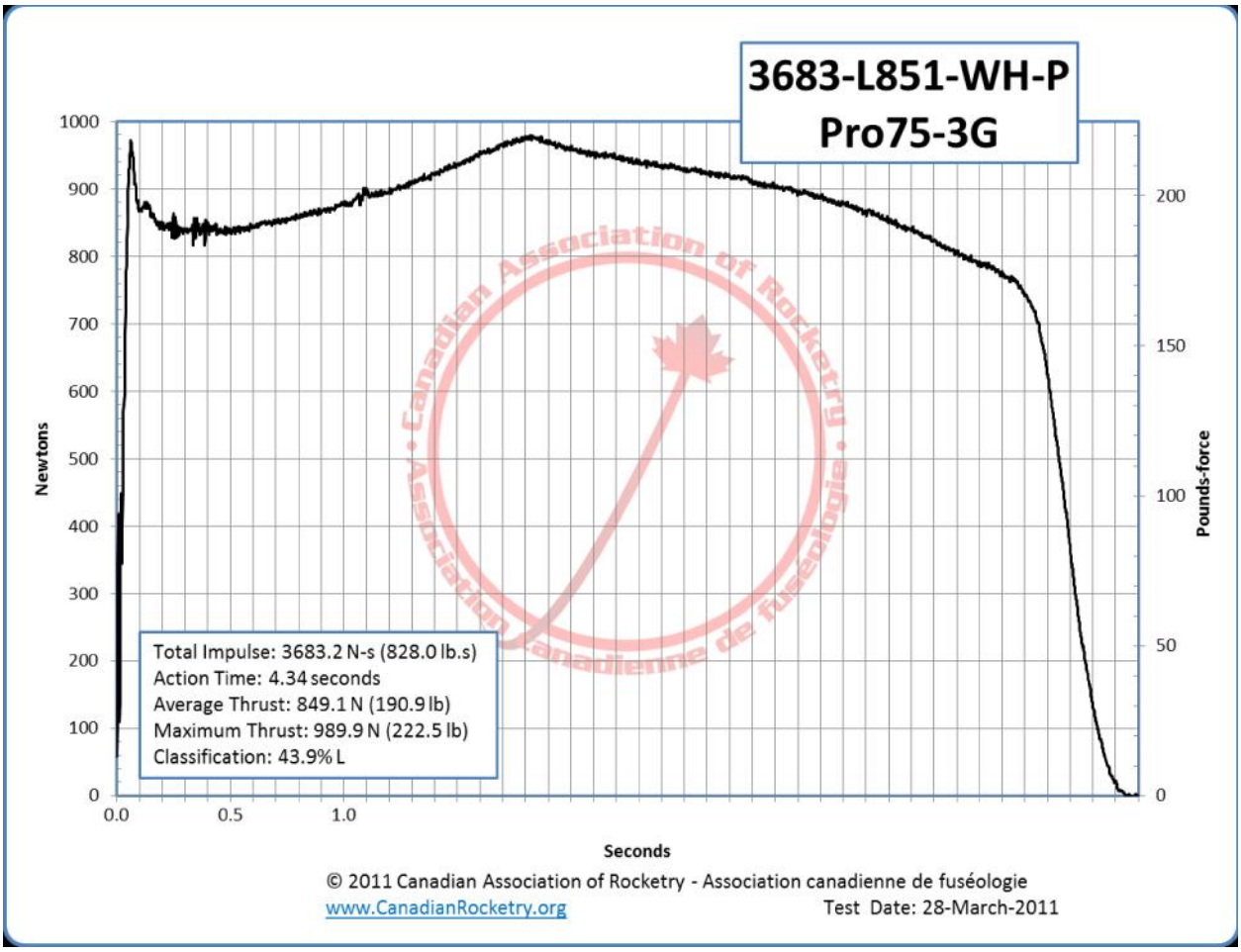

Figure 3.1.2 Thrust Curve for L851 [1]

The L851 has the least variation in its thrust, Figure 3.1.2, from ignition to thrust off the pad to flight, 20 lb and 10 lb, respectively. The motor will actually achieve max thrust during the flight which is an excellent characteristic. The time off the launch rail simulated is 0.40 sec. The actual time off the launch rail from the flight at Talladega was about 0.35 sec, which is reasonable with an error margin of 0.05 sec. The pre-payload safety change simulated altitude was 4874 ft wind, with an altitude of 5415 ft achieved at Talladega, AL. The atmospheric conditions will be discussed in Section 3.1.1.

The L1050 is the second most efficient motor studied, 54.05%, and is the second least variant in its thrust curve. It provides the third highest max thrust. The burn time is 3.56 sec which is the third longest but still significantly longer than 1.03 sec.

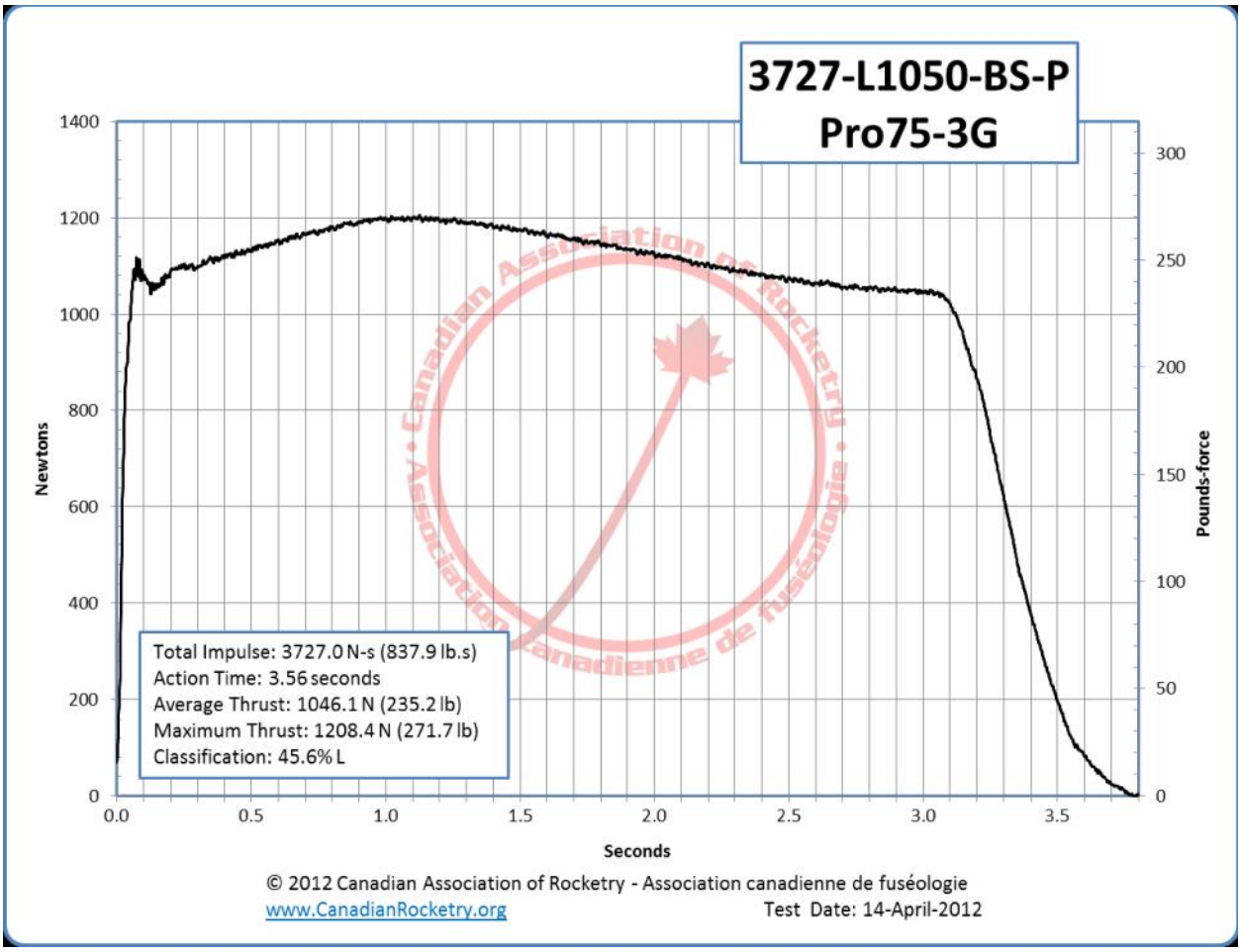

Figure 3.1.3 Thrust Curve for L1050 [1]

The L1050 varies in its thrust, Figure 3.1.3, from ignition to thrust off the pad to flight, 5 lb and 40 lb, respectively. The motor will achieve max thrust during flight. The time off the launch rail simulated is 0.40 sec. There is no actual flight data available as the L1050 was not tested on the ARES launch vehicle. Therefore, the variation in its actual flight characteristics compared to its simulated profile is not available.

The L800 is the third most efficient motor available, 53.35%, and is the third least variant in its thrust curve. Only the L3200 is more variant in its thrust than the L800. It provides the second highest max thrust. The burn time is the longest of all the motors selected for the study, 4.67 sec, with a difference of 0.33 sec from the next closest motor in burn time.

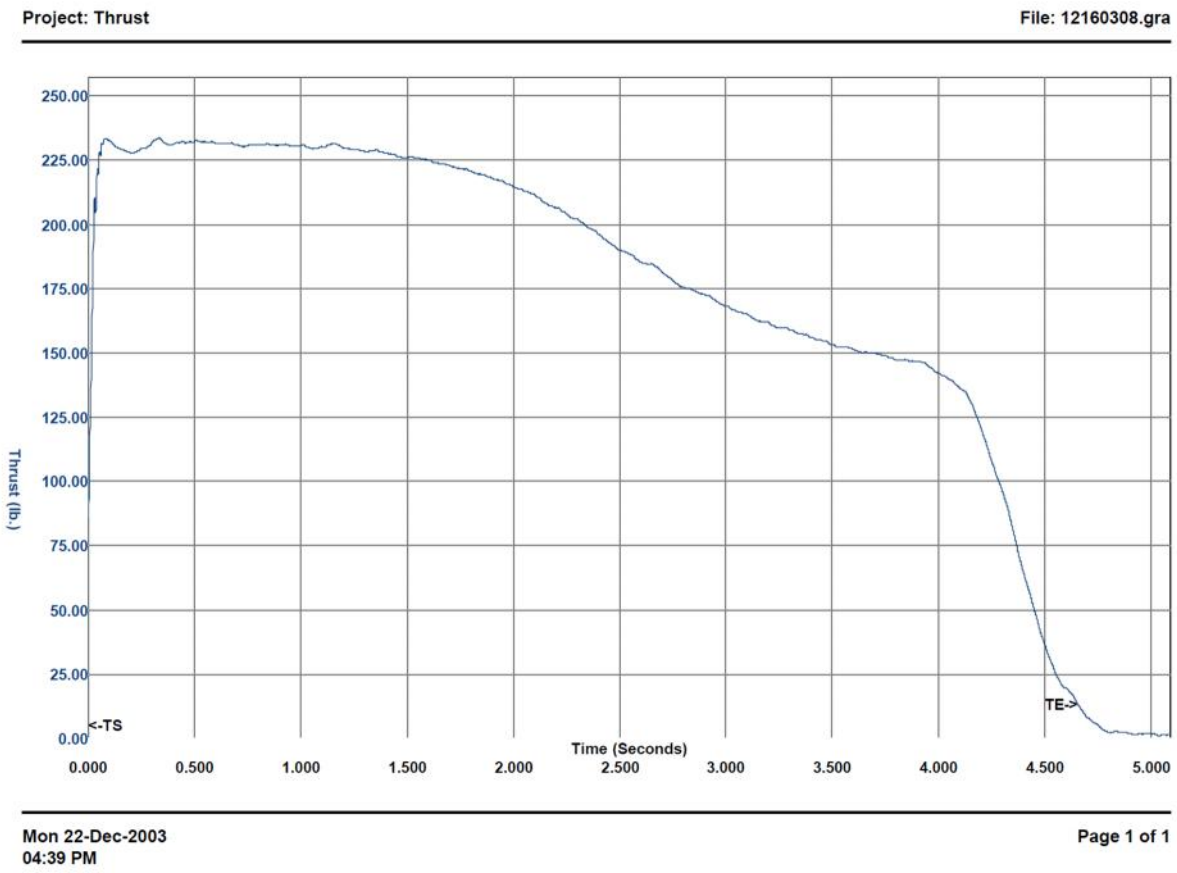

Figure 3.1.4 Thrust Curve for L800

As can be observed from the thrust curve, Figure 3.1.4, the L800 achieves its max thrust almost immediately off the pad. It is also an older motor as evidenced by the December 2003 test date. That does not necessarily imply reliability as use statistics are not available. The variation in thrust from ignition to off the pad to flight, 5 lb and 75 lb, respectively, is more acceptable than the L3200 because the variation occurs over a longer period of time. The time off of the launch rail is simulated at 0.44 sec, which puts the motor a little past its max thrust. There is no actual flight data available as the L1050 was not tested on the ARES launch vehicle. Therefore, like the L1050, the variation in actual flight to simulation is not available for study.

3.1.1 Atmospheric Data

Date	Location	0 ft	3,000 ft	6,000 ft
February 20	Talladega, AL	10 mph	30 mph	15 mph
March 5	Manchester, TN	5 mph	15 mph	20 mph

Table 3.1.2 Atmospheric Conditions During Full Scale Flight Tests [2]

The data from Table 3.1.2 was obtained through the Aviation Weather Center, (AWC) [2]. The Aviation Weather Center provides the wind speed in knots. The conversion from knots to mph is 1 knot to 1.15077945 mph.

3.1.1.1 L851 Flight

The L851 flight launch rail was angled to account for the wind at the launch site. With the long burn time of the L851 the motor was able to control the rocket's flight profile to apogee. The static stability throughout the flight and T/W ratio continually increased making maintaining the flight profile relatively simple.

3.2.1.2 L3200 Flight

The L3200 flight launch rail was angled to reduce the relative angle of attack, like the L851. With the short burn time and relatively little wind the launch vehicle was able to coast to its apogee of 4876 ft. The static stability at burnout is fixed on the launch vehicle.

3.2 Thrust off the Pad

In order to determine the mass rate loss or propellant mass burned throughout the flight the thrust equation, Eqn. 1 [3], is examined.

$$T = \frac{d}{d} v + (P_e \quad - P_{a\iota} \;)A_e \qquad \text{Eqn. 1}$$

Assumptions:

1. The exit pressure is equal to the atmospheric pressure.
2. The effective exhaust velocity is assumed to be uniform and constant.

The mass loss, dm/dt, can be determined through analyzing the thrust curves provided by [1]. The behavior of the thrust curve allows for the determination of how the mass rate will act, Table 3.2.1.

Thrust Curve Behavior	Mass Rate Loss Behavior
Constant	Linear
Linear	Quadratic
Quadratic	Cubic

Table 3.2.1 Mass Rate Loss Indicator

The thrust curves [4] are shown over time in Fig. 3.2.1. The data points were taken from [4] and plotted over time in MATLAB. It can be assumed that the L851 is a constant plot. The L3200, the L800, and the L1050 are assumed piecewise linear plots.

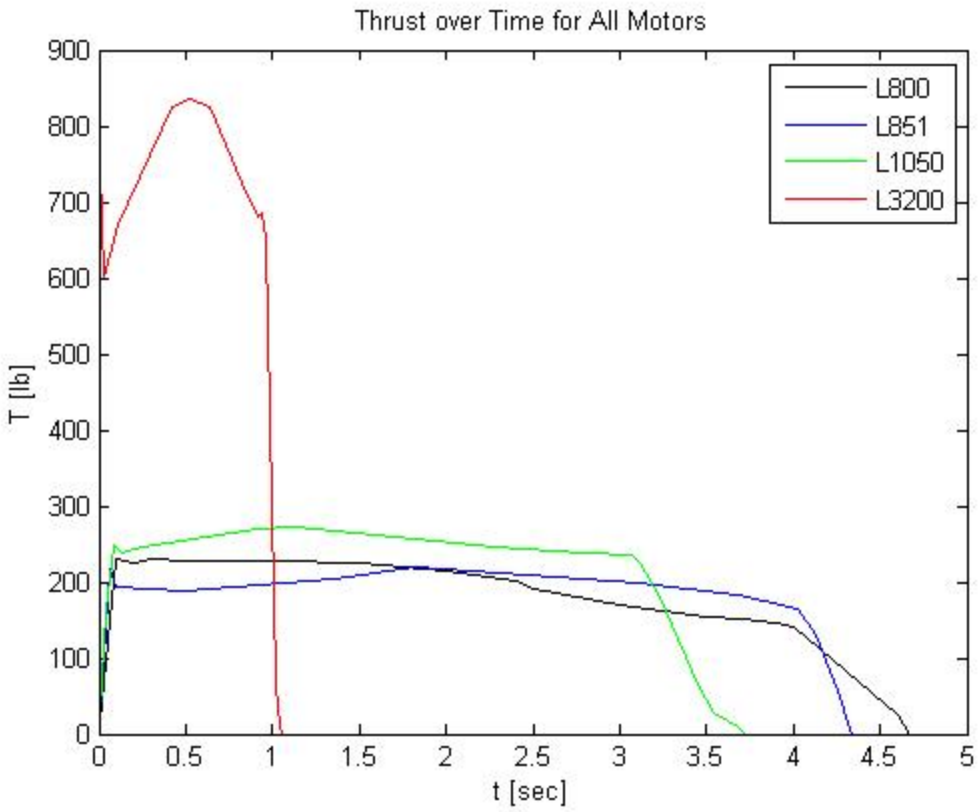

Figure 3.2.1 Thrust Curve of All Motors Considered Over Time

From these behaviors ARES observes the loss of propellant mass in the following fashion: Mass of propellant loss for L851 is a linear plot. The L3200 propellant loss plot is quadratic, linear, and quadratic. The L1050 is linear and then quadratic. The L800 is linear, quadratic, linear, and quadratic.

Using exported simulation data from OpenRocket the loss of propellant mass is observed in Figure 3.2.2. The exported data does not match the assumptions made from the thrust curves in Figure 3.2.1. The data seems to indicate that a quadratic function is used to interpolate between the initial and final mass of the propellant. [6] does not give an indication as to how the propellant mass change is approximated. Instead [6, p.66] explains how OpenRocket assumes that the mass moment of inertia changes from weight loss.

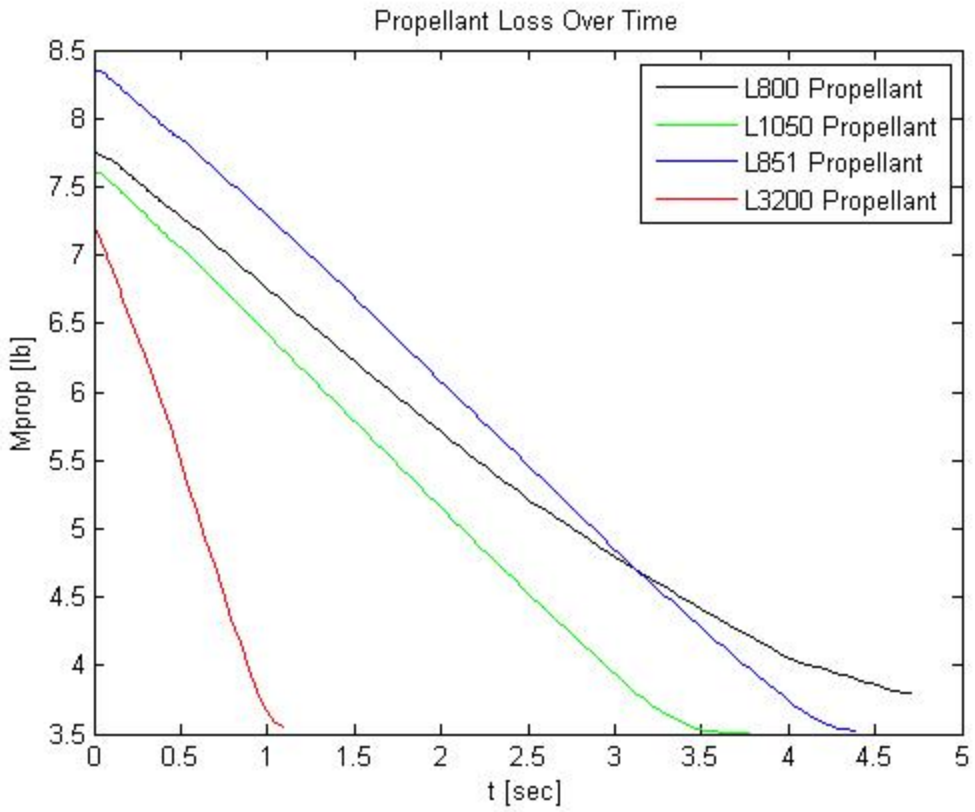

Figure 2.2.2 Mass of Propellant Loss over Time from OpenRocket

From these losses the overall weight of the launch vehicle will change throughout the burn and will then remain constant until apogee. At this point in the flight the static stability margin is no longer under consideration because the launch vehicle has left normal flight and begun the recovery phase.

3.2.1 Weight throughout Flight

The weight of the launch vehicle during powered-flight will decrease throughout the flight until motor burnout. An examination of the weight loss through the flight profile until apogee is provided in Figure 3.2.1.1.

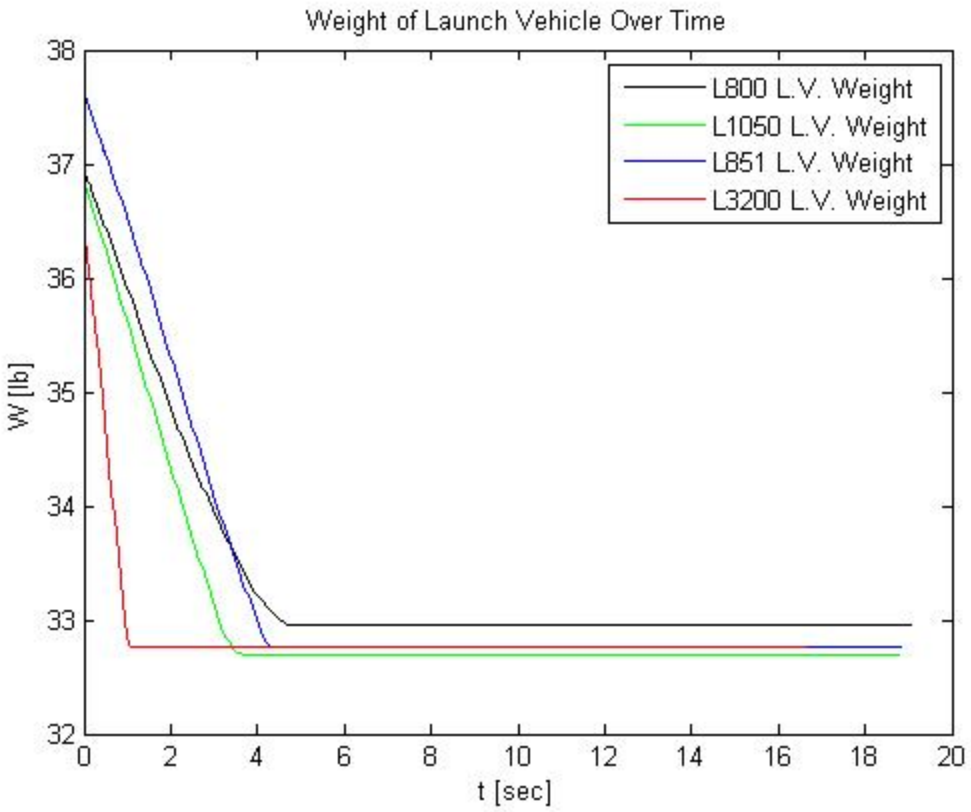

Figure 3.2.1.1 Weight Change of Launch Vehicle Under Each Motor Until Apogee

Motors	Launch Vehicle Initial [lb]	Launch Vehicle Final [lb]
L3200	36.4	32.8
L851	37.6	32.8
L1050	36.8	32.7
L800	36.9	32.9

Table 3.2.1.1 Initial and Final Weight of Launch Vehicle Under Each Motor

3.2.2 CG and Static Stability Margin throughout Flight

A change in weight will affect the CG positively as it will move up towards the nose cone creating a more favorable static stability margin. The pitching moment maximum for the longitudinal stability [5] able to be exerted to correct the flight path is shown in Eqn. 2.

$$M_C = L_C \; x \qquad \text{Eqn. 2}$$

The total lift acting at the center of pressure, CP, location gives the longitudinal pitch moment maximum, M_C , where the moment arm, x, is the distance between the CP location and the CG

location. From Eqn. 2 the static stability margin can be found as the moment arm or the distance between the CP location and the CG location, Eqn. 3. It is generally agreed that a stability margin of at least 2 calibers, (body diameters), will result in an adequately stable missile in the static sense [5].

$$x = x_C - x_C \quad \text{Eqn. 3}$$

$$S \quad M \quad = \frac{x}{d} \quad \text{[calibers]} \quad \text{Eqn. 4}$$

Where d is the maximum body diameter of the launch vehicle.

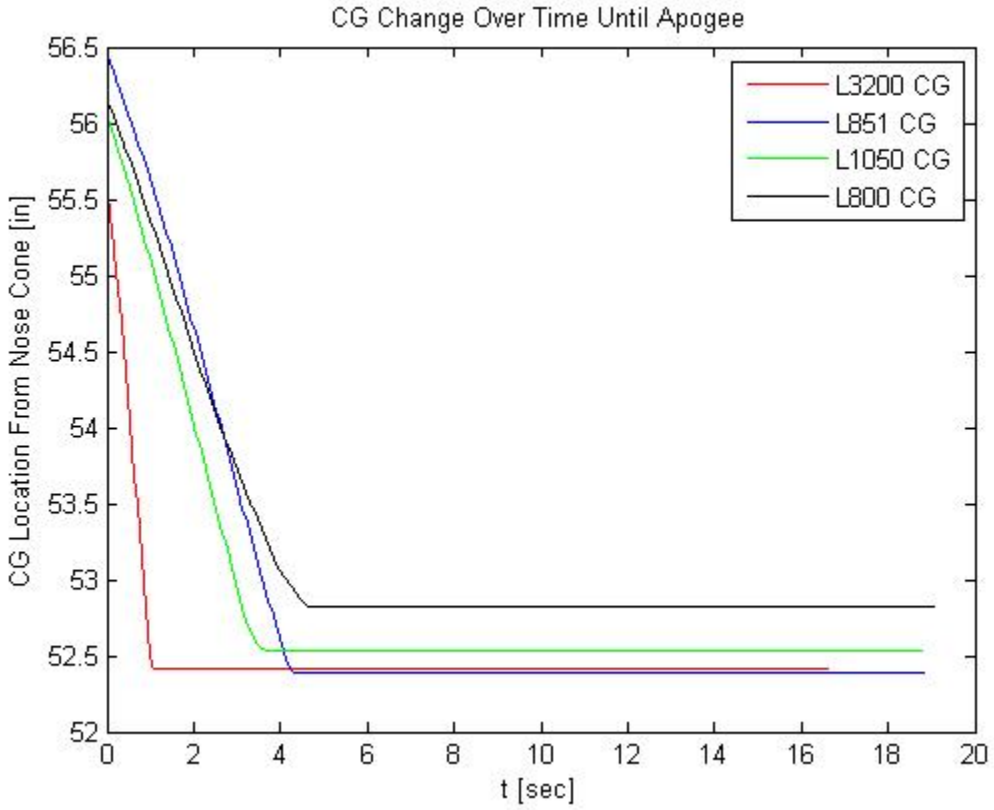

Figure 3.2.2.1 CG Location Change with Respect to the Nose Cone until Apogee

Due to the size of the motors there is some variance in the total weight loss and CG location change. For example; the L851 CG location moves further forward than the L3200 CG location despite having the same final weight [6, p. 66].

Motor	Initial CG Location [in]	Pad CG Location [in]	Final CG Location [in]
L3200	55.56	55.03	52.41
L851	56.22	55.84	52.39
L1050	56.03	55.68	52.53
L800	56.13	55.80	52.82

Table 3.2.2.2 CG Distance from the Nose Cone

In order to compare the static stability margin change and consider angles of attack, α, of up to 15 deg. Galejs' correction [7] to Barrowman's equations [8] were used. OpenRocket [6, p. 22] uses Barrowman's equations with a correction term of $\sin\frac{\alpha}{\alpha}$, which is comparable to Galejs' correction.

Motor	Stability Margin Off Rail [Calibers]	Stability Margin After Burnout [Calibers]
L3200	2.18	2.66
L851	2.04	2.66
L1050	2.06	2.64
L800	2.04	2.59

Table 3.2.2.3 Static Stability Margin Using [7] *for Off the Rail and After Powered Flight Phase*

From Table 3.2.2.3 the static stability margin, (SSM), off the rail is about the same for any slow-burning motor. For a fast-burning motor the SSM is higher because of its quicker loss of mass. As one of the three safer motors the L851 provides the best SSM. At burnout the L851 has increased the SSM to 2.66 calibers which matches the L3200's burnout SSM.
NAR actually recommends a maximum to the SSM off the rail to prevent over-stabilization, (dynamic instability), also commonly referred to as weather-cocking. "A maximum static stability margin of 3 calibers measured at an $\alpha$of 15 degrees and an airspeed corresponding to the lowest forward velocity at which the rocket is expected to leave the launcher guidance … should be used to protect against weathercocking," [12, p. 7].

3.2.3 T/W Ratio throughout Flight

The thrust to weight ratio, (T/W), has a required minimum of 3 by NAR. "...[The] rocket will not weigh more at liftoff than one-third of the certified average thrust of the high power rocket motor(s) intended to be ignited at launch," [9]. Tripoli Rocketry Association agrees, "Make sure that the initial thrust of the motor chosen will provide at least a 3:1 thrust-to-weight ratio (higher is better)," [10, p. 12]. Tripoli recommends discovering the thrust-to-weight ratio in one of two ways:

1. Initial thrust compared to the Gross Lift-Off Weight, (GLOW), of the rocket.
2. Peak thrust of the motor can be assumed to be at least equal to the average thrust as indicated in the motor designation. The average Newtons produced by the motor are then converted to pounds and compared to the GLOW of the rocket.

The 3:1 thrust-to-weight ratio is reiterated in Tripoli's, *Safe Launch Practices*. "The maximum lift-off weight of a rocket shall not exceed one-third (1/3) of the average thrust on the motor(s) intended to be ignited at launch," [11]. ARES was unable to find any documentation supporting a recommended T/W of 5 from NAR or Tripoli. ARES was also unable to find any documentation other than [5] suggesting a SSM of 2.00 calibers but agrees that both a T/W and a SSM approaching 5 and 2 calibers, respectively, create a good safety margin for the launch vehicle design.

Motor	T_avg./W_i	T_max/W_i	T/W Off Rail
L3200	19.8	23.0	16.75
L851	5.10	5.92	5.71
L1050	6.39	7.38	5.96
L800	4.89	7.83	5.29

Table 3.2.3.1 T/W for All Motors Considered in the Study

From the values in Table 3.2.3.1 it can be observed that unless the motor is a fast-burning highly reactive motor the T/W will fall around 5 for the ARES launch vehicle. The L3200 would appear to place undue stress on the launch vehicle. From the simulation data the L1050 provides the best T/W spread but is not flight tested. Thankfully, the L851 is flight tested under atmospheric conditions and is the second best over the T/W spread.

3.2.4 History of Each Motor Considered

The history of motor CATO's are not public and the team was unable to take into account the motor history in the decision. Instead ARES examined "Launching Safely in the 21st Century," [12, p. 12]. Performing a statistical analysis of flight failures, incidents, and accidents it was discovered that about 30% of all failures for simple rockets were in the powered flight phase.

A catastrophic rocket motor malfunction ("CATO") was experienced by both University of Alabama at Huntsville and Auburn University from bonded motors. ARES observed these CATO's and was frightened to use the L3200 because it requires bonding and is a highly-reactive fast-burning motor. This would be a secondary factor, "Improper assembly of reloadable motor," which would cause motor CATO.

Hazard	**Proximate Causes**	**Secondary Factors**	**Root Causes**	**Potential Mitigation**
Catastrophic rocket motor malfunction ("CATO")	1. Motor failure 2. Igniter positioning or improper igniter	1. Launch cables too short to support HPR distances 2. Improper assembly of reloadable motor 3. Improper storage of motor 4. Error in manufacturing (e.g. propellant voids)	Chamber pressure exceeds limits of motor hardware as assembled	1. Pad-person distance based upon actual failure data 2,3. Education on handling and storage procedures 4. Motor certification and failure reporting system

Table 3.2.4.1 Breakdown of Motor CATO [12, p. 15]

3.2.5 Requirements on Trajectory/Launch of Launch Vehicle

The trajectory/launch of the launch vehicle:

1. The rocket will be launched away from the flight line. Weather-cocking will be taken into account so that the rocket does not head towards the flight line when launched, [10, p.12].
2. The rocket will not be launched if ground level winds exceed 20 mph, [10, p.8].
3. The rocket will not be launched if the planned flight path will carry the vehicle through any clouds, [10, p.8].
4. The rocket will be launched from a stable device that provides rigid guidance until the rocket has reached a speed adequate to ensure a safe flight path, [9, 11].
5. The rocket will not be launched at an angle more than 20 degrees from vertical, [9, 11].
6. The stability of the rocket will be checked prior to flight and will not fly if it cannot be determined to be stable, [9].
7. The rocket will not exceed any applicable altitude limit in effect at that launch site, [9-11], 5600 ft at Bragg Farms.

3.2.6 Trajectory and Velocity of the Launch Vehicle Leaving the Rail

Powered flight instability is responsible for roughly 20% of hobby rocket failures. Rockets without thrust vector or active aerodynamic surface control of their trajectory must rely upon designs which allow the rocket to fly straight and true after leaving the launcher, [12, p. 30]. The ARES launch vehicle does not have active trajectory control.

There exist a number of conditions under which the commonly-used measures of static stability may lead to hazardous flight paths. The ARES team uses OpenRocket and Galejs' corrections to Barrowman's equations, [6, 7]. "Rockets must be guided by launch rods, rails, or towers until they have attained a forward velocity of at least 4 times the velocity at which the wind is blowing or gusting at the launch site," [12, p. 7]. The rocket must leave the launch system with sufficient velocity to allow the restoring torque provided by the fins, assuming the fins are the source of the corrective pitch moment, to overcome disturbances. NAR recommends 4 times the velocity at which the wind is blowing based on experience. The assumption is made that the launch rod is sufficiently rigid that "rod whip" does not disturb the rocket as it exits the system, [12, p. 31]. The ARES team observed rod whip on the L3200 launch but was unaware at the time that this was an assumption made to calculate the relative angle of attack. Therefore, the L3200 information is relative to the flex of the launch rod system.

Motor	Rail Exit Velocity [ft/s]
L3200	168.00
L851	121.16
L1050	124.23
L800	126.91

Table 3.2.6.1 Rail Exit Velocity on 12 ft Rail for Each Motor

Wind Speed	5 mph (7.33 ft/s)	10 mph (14.67 ft/s)	15 mph (22 ft/s)	20 mph (29.33 ft/s)
L3200 AOA	0.00 deg.	0.00 deg.	2.46 deg.	4.90 deg.
L851 AOA	0.00 deg.	1.90 deg.	5.29 deg.	16.8 deg.
L1050 AOA	0.00 deg.	1.73 deg.	5.04 deg.	16.6 deg.
L800 AOA	0.00 deg.	1.60 deg.	4.83 deg.	17.6 deg.

Table 3.2.6.2 Relative Angle of Attack in Degrees with Launch Rod Tilted to ±5 deg.

Table 3.2.6.2 was calculated from the data from OpenRocket simulations and real data available from the full scale launch test flights presented in Table 3.2.6.1. Based off the observed rod whip for the L3200, ARES suspects because of the high thrust, the relative angle of attack calculated for the L3200 is considered nominal. The other motors in the study all remain under the maximum 20 deg. relative angle of attack. L851 and L1050 show the best results at the maximum ground wind speed.

The relative angle of attack is important to consider when examining the dynamic stability of the rocket. The static stability margin describes the ability of the rocket to create a corrective pitching moment. A large degree of static stability will cause a large aggressive response to any wind and will potentially lead to dynamic instability. This idea is illustrated in Figure 3.2.6.1.

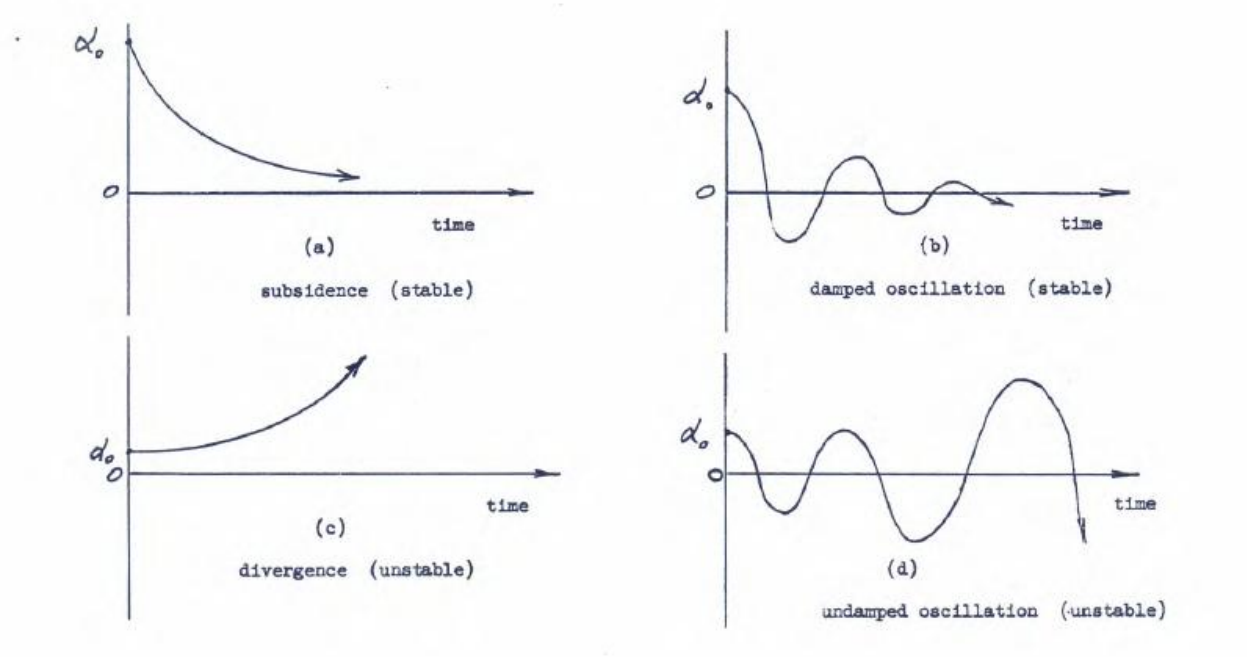

Figure 3.2.6.1 (a) Shows a statically stable system, (b) Shows a dynamically stable system (c) Shows a statically unstable system, (d) Shows a dynamically unstable system [5]

NAR says, "If the rocket…does not have a high initial thrust-to-weight ratio it may follow a parabolic trajectory and impact the ground (or a person or vehicle) under power. This behavior is sometimes referred to as a 'gravity turn,'" [12, p. 32]. This statement is only true under the consideration that the velocity provided by the thrust, when higher, lowers the relative angle of attack. There is no ability of the thrust to produce a pitching moment unless incorrect construction procedures were followed and the motor was not centered in the body.

3.2.7 Altitude Data for all Motors

Motor	Original Simulation Altitude [ft]	Option 1 Simulation Altitude [ft]	Real Flight Test Altitude [ft]
L3200	4566	4684	4876
L851	4874	5018	5415
L1050	5170	5311	N/A
L800	5069	5215	N/A

Table 3.2.7.1 Motor Altitude Data

The simulation altitudes and real flight test altitudes can be seen above in *Table 3.2.7.1*. The percent difference between original simulation altitude and the real flight test data for the L3200 and L851 was 6.36% and 9.99%, respectively. Applying these expected altitude variances to the Option 1 simulations of the L1050 and L800 would predict their actual flight altitudes above the allowable 5600 ft. This makes the L1050 and L800 not viable motor options for altitude safety reasons.

4. Conclusion

The ARES Team is truly convinced based on the research shown and the data from their test flight that the Cesaroni L851 is the safest option for the team to launch on. As was shown in this report, the L851 is a favorable option compared to the other available motors, the L800 and L1050. In addition, this motor has already been successfully tested with the ARES launch vehicle which provides an invaluable amount of confidence in the L851. The ARES Team is determined to have a safe launch, and believes that the Cesaroni L851 is the motor that is most capable of providing just that.

References

[1] “Motor Data,” Cesaroni Technology Incorporated [online], http://www.pro38.com/products/pro75/motor.php [retrieved April 4, 2016].

[2] “ADDS Wind Temp Data,” Aviation Weather Center, NOAA, National Weather Service [online], https://www.aviationweather.gov/windtemp [retrieved 20 February and 4-5 March 2016].

[3] Humble, R.W., Henry, G. N., and Larson, W. J., “Introduction to Space Propulsion,” *Space Propulsion Analysis and Design,* 1st ed. Revised, McGraw-Hill, 1995, pp. 9-19.

[4] “ThrustCurve Hobby Rocket,” *ThrustCurve.org*, [online database], http://www.thrustcurve.org/index.shtml, [retrieved 9 April 2016].

[5] Gurkin, L.W., “Basic Missile Aerodynamic Stability,” *National Association of Rocketry*, NASA, August 1964, pp. 11-13.

[6] Niskanen, S. “Chapter 4: Flight simulation, Section 2: Modeling rocket flight, Subsection 3: Mass and moment of inertia calculations,” *OpenRocket technical documentation: For OpenRocket version 13.05*, 10 May 2013.

[7] Galejs, R. “Wind Instability: What Barrowman Left Out,” *High-Powered Rocketry*, September 1998.

[8] Barrowman, J.S., and Barrowman, J.A., “The Theoretical Prediction Of The Center Of Pressure,” NARAM-8, 1966 August 18.

[9] “High Power Rocket Safety Code,” National Association of Rocketry [online], http://www.nar.org/safety-information/high-power-rocket-safety-code/, [retrieved 9 April 2016].

[10] “Range Safety Guidelines,” Tripoli Rocketry Association v1.3, 12 November 2015.

[11] “Safe Launch Practices,” Tripoli Rocketry Association, July 2013.

[12] “Launching Safely in the 21st Century,” National Association of Rocketry, Final Report of the Special Committee on Range Operation and Procedure, 29 October 2005.